Journal of Physics and Chemistry of Solids 74 (2013) 1683–1685

Contents lists available at ScienceDirect

Journal of Physics and Chemistry of Solids

journal homepage: www.elsevier.com/locate/jpcs

Temperature-dependent photoreflectance of SnS crystals

T. Raadik*, M. Grossberg, J. Raudoja, R. Traksmaa, J. Krustok

Tallinn University of Technology, Ehitajate tee 5, 19086 Tallinn, Estonia

ARTICLE INFO

Article history:
Received 14 December 2012
Received in revised form
24 May 2013
Accepted 5 June 2013
Available online 15 June 2013

Keywords:
A. Photoreflectance
A. Solar cells
A. Solar energy materials

ABSTRACT

The optical properties of single-crystal SnS were studied by photoreflectance (PR) spectroscopy. Temperature-dependent PR spectra were measured in the range 20–200 K. A room-temperature bandgap energy value of $E_g = 1.317$ eV was estimated by fitting the temperature dependence of the bandgap energy obtained from the PR spectra. The vibrational properties of orthorhombic SnS were studied using Raman spectroscopy. Four vibrational modes were detected at 95, 163, 191, and 218 cm^{-1}.

1. Introduction

Orthorhombic tin monosulfide (SnS) thin films have attracted much attention because of their suitability for solar energy cells with properties such as a direct optical bandgap [1–3], p-type conductivity, and a high absorption coefficient of 10^4–10^5 cm^{-1} [2,3]. SnS, a group IV–VI semiconductor, is a cheap and abundant material with low toxicity. Theoretical calculations revealed conversion efficiency of up to 25% for SnS photovoltaic devices [4]. The highest value reported so far for an inorganic–organic heterojunction solar cell based on SnS-sensitized mesoporous spherical TiO_2 electrodes is 2.8% [5]; however, thin-film SnS solar cells have shown efficiency of only ~2.04% [6].

Although the optical properties of SnS have been studied for over 30 years, there are still some open questions. The room-temperature bandgap energy reported for SnS varies in the range 1.1–1.87 eV and the correct value is still unclear [1–3,7]. Kim and George investigated SnS epitaxial films grown by atomic layer deposition on glass substrates and found a bandgap energy of $E_g = 1.87$ eV [1]. Reddy et al. calculated bandgap energy of $E_g = 1.47$ eV from transmittance spectra for SnS films prepared by thermal evaporation [2]. SnS films deposited by chemical bath deposition had bandgap energies of 1.75 and 1.12 eV for zinc blende and orthorhombic structures, respectively [3]. Lambros et al. found bandgap energies of 1.14 and 1.10 eV for SnS single crystals from absorption and reflectance spectra, respectively [7]. Large differences in the bandgap values could be caused by other phases such as SnS_2 and Sn_2S_3 in the films, as described by Cheng and Conibeer [8], or by change in absorption edge due to an indirect transition at lower energy. Additional studies using controlled single-phase samples and different experimental methods are needed to solve these discrepancies.

Photoreflectance (PR) has been widely used as a general method for studying the optical and electrical properties of semiconductors [9]. Because it is non-destructive and requires no electrical contact, PR is one of the most useful among modulated spectroscopy techniques. Here we present PR data for monocrystalline SnS measured over a wide temperature range.

2. Experimental

SnS was synthesized from Proanalysi grade Sn and 3 N purity S. The precursors were mixed and sealed in an evacuated quartz ampoule and inserted into a furnace. The furnace was slowly heated to 700 °C over 100 h and then kept at that temperature for 24 h before cooling to room temperature. The resulting polycrystals were then sealed in an evacuated ampoule for sublimation. The part of the ampoule in which the SnS powder was located was kept at ~650 °C and SnS single crystals grew in the part at a lower temperature zone of 620 °C. The sublimation process was allowed to run for 3 weeks. The single SnS crystals obtained had a plate-like shape with a good reflecting surface and were approximately 3 mm × 3 mm in size.

Raman spectral measurements were made at room temperature on a high resolution micro-Raman spectrometer (Horiba JobinYvon HR800) equipped with a multichannel CCD detection system in the backscattering configuration. An Nd-YAG laser ($\lambda = 532$ nm) with a spot size of 10 μm in diameter was used for excitation. X-Ray diffraction (XRD) measurements were performed using a Bruker D5005 diffractometer (Bragg–Brentano geometry) with Cu $K_{\alpha 1}$ radiation ($\lambda = 1.5406$ Å) at 40 kV and 40 mA and a

* Corresponding author. Tel.: +372 620 3210; fax: +372 620 3367.
E-mail address: taavi.raadik@ttu.ee (T. Raadik).

0022-3697/$ - see front matter © 2013 Elsevier Ltd. All rights reserved.
http://dx.doi.org/10.1016/j.jpcs.2013.06.002

graphite monochromator. The ICDD PDF-4+2012 database was used for identification. The XRD pattern obtained for an SnS monocrystal is shown in Fig. 1. All the XRD peaks closely match those for orthorombic SnS. Lattice constants of $a=1.1200$ nm, $b=0.3980$, and $c=0.4320$ nm were obtained for the crystal.

PR measurements were made using a traditional setup [9] with a 40-cm grating monochromator and a 250-W halogen bulb as the primary beam and a 51-mW solid-state laser ($\lambda=405$ nm) as the secondary beam. The reflectance signal at 85 Hz was detected using a Si detector and a lock-in amplifier. The single crystals investigated were glued onto the cold finger of a closed-cycle He cryostat with cryogenic grease.

3. Results and discussion

Four main peaks are evident in the Raman spectra (Fig. 2). The most intense peak is at 191 cm^{-1} and the others are at 95, 163, and 218 cm^{-1}. According to the literature, these can be attributed to orthorombic SnS [8,10,11]. The presence of additional phases could not be detected from the Raman data. The Raman spectra were fitted using Lorentzian functions to resolve the peaks. The lattice vibrations at 95, 191 and 218 cm^{-1} correspond to the A_g modes, and the peak at 163 cm^{-1} to the $B_{3\,g}$ mode of SnS [10].

PR spectra at three different temperatures are shown in Fig. 3 for measurements in the temperature range 20–200 K. As the temperature increases, the PR signal shifts to lower energy and decreases in intensity, as observed from the scale factors.

Each PR spectrum was analyzed by fitting the data to a low-field line-shape function with a third-derivative functional form [12]:

$$\Delta R/R = \mathrm{Re}\left[Ae^{i\varphi}(E-E_g+i\Gamma)^{-m}\right], \quad (1)$$

where E is the photon energy, A is the amplitude, φ is the phase, E_g is the bandgap energy, and Γ is the spectral broadening parameter. The exponent m depends on the type of critical point and determination of a suitable value is of particular importance in analyzing PR spectra. A value of $m=3$, corresponding to a two-dimensional critical point, did not give a good fitting result. Therefore, $m=2.5$, corresponding to a three-dimensional critical point, was used for PR spectral fitting since this yielded an excellent fit for the majority of our data.

The temperature dependence of the bandgap energy obtained by fitting the PR spectra to Eq. (1) is plotted in Fig. 4. Experimental data were fitted to the O′Donnell expression [13]

$$E_g(T) = E_g(0) - S\langle\hbar\omega\rangle\left[\coth\left(\langle\hbar\omega\rangle/2kT\right)-1\right], \quad (2)$$

where $E_g(0)$ is the bandgap energy at 0 K, S is a dimensionless coupling constant, and $\langle\hbar\omega\rangle$ is the average phonon energy. The fitting parameters obtained were $E_g(0)=1.375\pm0.001$ eV, $S=1.86\pm0.21$ and $\langle\hbar\omega\rangle=24.3\pm3.0$ meV. By extrapolating the fitting result to the O′Donnell equation for higher temperatures it is possible to estimate the bandgap energy at room temperature, resulting in $E_g=1.317$ eV. The average phonon energy of $\langle\hbar\omega\rangle=24.3$ meV $=196\ cm^{-1}$ is very close to the value of 191 cm^{-1} measured by Raman spectroscopy (Fig. 2).

Fig. 4 shows the temperature dependence of the bandgap energy for SnS obtained by Parenteau and Carlone [14] for comparison. The comparison reveals differences in bandgap energy values and their temperature-dependent behavior. Different samples and

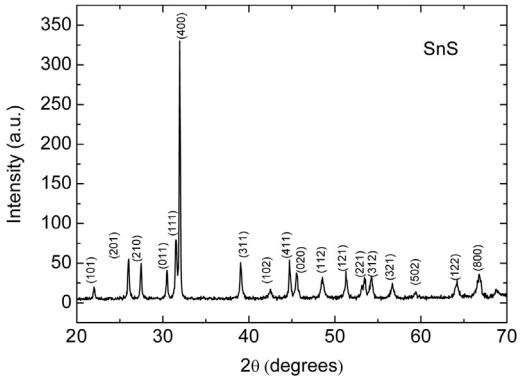

Fig. 1. XRD pattern for SnS monocrystals.

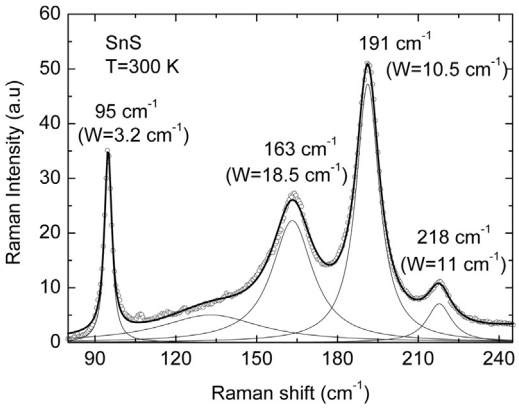

Fig. 2. Room-temperature Raman spectrum for single-crystal SnS.

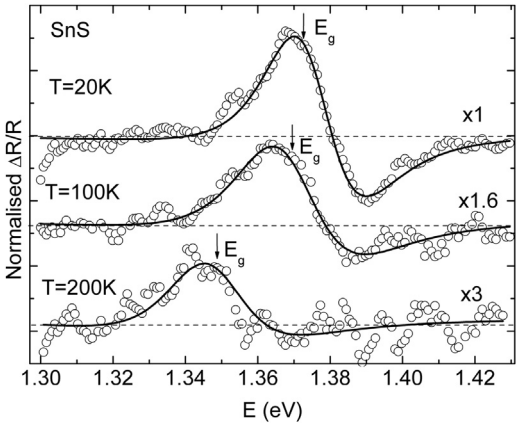

Fig. 3. Temperature-dependent PR spectra for single-crystal SnS. Circles show experimental results and continuous lines are the fitting results according to Eq. (1).

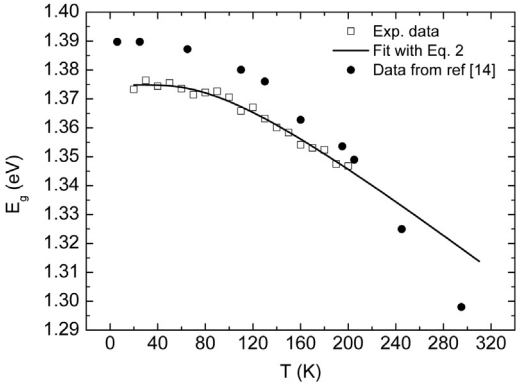

Fig. 4. Bandgap energy values for single-crystal SnS determined by fitting the PR spectra as a function of temperature, the data fit to Eq. (2), and data reported by Parenteau and Carlone [14].

measurement methods could be the reason for this discrepancy. Parenteau and Carlone used optical absorption for bandgap studies [14] while we used PR. These disparities confirm the need for further studies of the properties of SnS.

4. Conclusion

PR of monocrystalline SnS was investigated in the temperature range 20–200 K. The PR data obtained were analyzed by fitting the spectra to a low-field line-shape function, from which the bandgap energy at different temperatures was determined. The temperature dependence of the bandgap energy was fitted using the O′Donnell expression. The O′Donnell model gives a room-temperature bandgap estimate of 1.317 eV.

Acknowledgements

This research was supported by Estonian Science Foundation grants 8282 and 9369, target financing by the Estonian Ministry of Education and Research (No. SF0140099s08), the Estonian Centre of Excellence in Research "High-Technology Materials for Sustainable Development" (project TK117T), the Estonian Governmental Program for New Energy Technologies (project AR 10128), and by graduate school "Functional Materials and Technologies" funding from the European Social Fund under project 1.2.0401.09-0079 in Estonia.

References

[1] J.Y. Kim, S.M. George, J. Phys. Chem. C 114 (2010) 17597–17603.
[2] N.K. Reddy, Y.B. Hahn, M. Devika, H.R. Sumana, K.R. Gunasekhar, J. Appl. Phys. 101 (2007) 093522.
[3] C. Gao, H. Shen, L. Sun, Z. Shen, Mater. Lett. 65 (2011) 1413–1415.
[4] R.H. Bube, Photovoltaic Materials, Imperial College Press, London, 1998.
[5] W. Guo, Y. Shen, M. Wu, T. Ma, Chem. Commun. (2012) 6133–6135.
[6] P. Sinsermsuksakul, K. Hartman, R.G. Gordan, Appl. Phys. Lett. 102 (2013) 053901.
[7] A.P. Lambros, D. Geraleas, N.A. Economou, J. Phys. Chem. Solids 35 (1974) 537–541.
[8] S. Cheng, G. Conibeer, Thin Solid Films 520 (2011) 837–841.
[9] T. Raadik, J. Krustok, M.V. Yakushev, Physica B 406 (2011) 418–420.
[10] H.R. Chandrasekhar, R.G. Humphreys, U. Zwick, M. Cardona, Phys. Rev. B 15 (1977) 2177–2183.
[11] S. Sohila, M. Rajalakshmi, C. Gosh, A.K. Arora, C. Muthamizhchelvan, J. Alloys Compd. 509 (2011) 5843–5847.
[12] D.E. Aspnes, in: M. Balkanski (Ed.), Handbook on Semiconductors II, North-Holland, Amsterdam, 1980, p. 109.
[13] K.P. O′Donnell, X. Chen, Appl. Phys. Lett. 58 (1991) 2924–2926.
[14] M. Parenteau, C. Carlone, Phys. Rev. B 41 (1990) 5227–5234.